Responses of Phytoplankton and Bacterial Metabolism to CO_2 Enrichment during a Bloom in a Coastal Mesocosm

Yibin Huang [†] [‡], Xin Liu[†] [‡], Edward A. Laws [§], Binzhang Chen [//], Yan Li[†], Yuyuan Xie [†] [‡], Yaping Wu [⊥],Kunshan Gao*[†], Bangqin Huang*[†‡]

[†] State Key Laboratory of Marine Environmental Science, Xiamen University, Xiamen, China.

[‡] Fujian Provincial Key Laboratory of Coastal Ecology and Environmental Studies, Xiamen University, Xiamen, China.

[§] Department of Environmental Sciences, School of the Coast and Environment, Louisiana State University, Baton Rouge, Louisiana, USA.

[//] Ecosystem Dynamics Research Group, Research and Development Center for Global Change, Japan Agency for Marine-Earth Science and Technology, Yokohama, Japan.

[⊥] College of Oceanography, Hohai University, Nanjing, China.

*E-mail: bqhuang@xmu.edu.cn; ksgao@xmu.edu.cn.

KEYWORDS: CO_2 enrichment, mesocosm, gross primary production, bacterial respiration, bacterial growth efficiency, net community production

[键入文字]

Abstract: Effect of ocean acidification (OA) on organisms and ecosystem services are increasingly recognized as an environmental issue both in the scientific community and the general public at global scale. Growing attentions are being paid to OA effects under multiple stressors or fluctuating environmental conditions in order to extrapolate from laboratory-scale experiments to natural systems. We operated a mesocosm experiment in a coastal water with an assemblage of three model phytoplankton species and their associated bacteria under the influence of elevated CO_2 concentrations. Net community production and the metabolic characteristics of the phytoplankton and bacteria were monitored to elucidate how these organisms respond to the CO_2 enrichment during the course of the phytoplankton bloom. We found that the CO_2 enrichment (1000 μatm) significantly enhanced gross primary production and the ratio of photosynthesis to chlorophyll *a* by approximately 38% and 39%, respectively, during the early stationary phase of the phytoplankton bloom. Although there were few effects on bulk bacterial production, a significant decrease of bulk bacterial respiration (up to 31%) at elevated CO_2 resulted in an increase of bacterial growth efficiency. The implication is that an elevation of CO_2 concentrations leads to a reduction of bacterial carbon demand and enhances carbon transfer efficiency through the microbial loop, with a greater proportion of fixed carbon being allocated to bacterial biomass and less being lost as CO_2. The contemporaneous responses of phytoplankton and bacterial metabolism to CO_2 enrichment significantly increased net community production by about 45%, an

increase that would have profound implications for the carbon cycle in coastal marine ecosystems.

Introduction

Increases of atmospheric pCO_2 due to human activities since the Industrial Revolution are known to have influenced organisms and the delivery of oceanic ecosystem services at a global scale.[1] Increasing dissolution of atmospheric CO_2 into the oceans leads to progressive ocean acidification (OA) and a shift in the distribution of inorganic carbon species in seawater.[2] The impacts of projected CO_2 emissions will likely induce a decrease of 0.3–0.4 in seawater pH by the end of this century.[3, 4] In coastal regions, the rate of decline of pH will likely be exacerbated due to the interactions between OA and other natural or anthropogenic processes.[5-7] In marine systems, phytoplankton and heterotrophic bacteria play a fundamental role in the carbon cycle; the former account for about half of global primary production,[8] and the latter play a vital role in recycling nutrients and organic matter through the microbial loops.[9] These two groups may be directly and indirectly affected by OA, with major implications for marine ecosystems and biogeochemical processes.[10, 11]

Studies of the direct effects of OA on marine phytoplankton physiology and community composition have focused particularly on diatoms, coccolithophores, and cyanobacteria.[12] The impacts of OA on phytoplankton metabolism are mainly linked to two processes: (1) energy savings due to down-regulation of CO_2-concentrating mechanisms (CCMs) under enhanced CO_2 and HCO_3^- availability,[13] and (2) increased demand for energy associated with maintenance of a constant intracellular pH as the extracellular pH declines.[14] Various studies have reported positive,[15-17] neutral,[18, 19] and negative [20, 21] effects of elevated CO_2 on phytoplankton growth rates and photosynthesis.

Relatively few studies have addressed the effects of elevated CO_2 on the metabolism of bacteria compared to phytoplankton, and those studies have tended to focus on bacterial production.[22] Heterotrophic bacterial activity is likely to be affected by changes in the supply of organic substrates associated with microalgal carbon fixation and exudation under elevated pCO_2 conditions [23, 24] and deceases of seawater pH.[25, 26] For example, stimulation of bacterial production, especially the part associated with the particle-attached bacteria, has been reported at high pCO_2, presumably because of the formation of more phytoplankton-derived particles, which serve as sites for bacterial attachment.[23] In contrast, Coffin, et al. [27] have reported a reduction of bacterial production within a deep-sea community at low pH due to the negative

effect of the low pH on cell integrity. However, to our knowledge, there have been few direct reports of the effects of OA on bacterial respiration, despite its important role in the carbon cycle. Teira, et al. [26] first examined the response of bacterial respiration to elevated CO_2 in a culture and reported a reduction of respiration. The authors speculated that this response may have been related to a reduction of energetic costs at high pCO_2 (1000 μatm); under these conditions the pH of the water (7.6) was similar to the intracellular pH of the bacteria.[26] However, little response of bacterial respiration to elevated CO_2 has been reported in a natural bacterial community of Artic ocean.[28] Therefore, effects of increased CO_2/lowered pH on heterotrophic bacterial metabolism are of general concern.

In this study, we used three phytoplankton species—*Phaeodactylum tricornuntum*, *Thalassiosira weissflogii*, and *Emiliania huxleyi*—and the bacterial flora from the algal cultures to carry out a coastal-water mesocosm experiment. The experimental design took into consideration the extensive database from laboratory studies of the responses of the selected species to OA and was designed as an intermediate and necessary step between laboratory-scale research and studies of highly complex natural communities. Compared with the relatively stable conditions in laboratory, the mesocsom approach is closer to the natural conditions, as reflected in multiple stressors or fluctuating environmental conditions such as solar radiation and varying

diurnal temperature. The mesocosm study involved a relatively simple artificial community composed of a few key species of phytoplankton and the bacteria that developed with the algal growth. The experimental design aimed to link the effects of OA in the laboratory researches with meso-scale studies, facilitating assessments of the responses of phytoplankton and their associated heterotrophic processes to CO_2 enrichment in the regional coastal waters. The dynamics of the inorganic carbon system in the mesocosms was determined by the continuous supply of CO_2 via areation and biological activity, therefore, mirroring that in natural phytoplankton blooms in coastal waters, where the carbon system is strongly influenced by biological process and air-sea gas exchange. We hypothesized that, 1) in nutrient-rich coastal waters, elevated pCO_2 might enhance phytoplankton primary production and that bacterial growth and production would be consequently stimulated; 2) these responses might collectively lead to a change of net community production. To test these hypotheses, we investigated the effects of CO_2 enrichment on net community production and the metabolic characteristics of phytoplankton and heterotrophic bacteria in a coastal mesocosm.

Materials and Methods

Experimental Setup

The mesocosm experiment was conducted on a floating platform at the Facility for the Study of Ocean Acidification Impacts of Xiamen University (FOANIC-XMU, 24°31′48″ N, 118°10′47″ E) in Wu Yuan Bay, Xiamen.[29] The experiment lasted from 22 December 2014 (day 0 with respect to algal inoculation) to 24 January 2015. Six cylindrical transparent thermoplastic polyurethane (TUP, 0.9 mm thick) bags were set up and submerged in the seawater along the southern side of the platform. Each mesocosm was about 1.5 m in diameter and 3 m deep, with 0.5 m projecting above the seawater. The volumes of the enclosures below the sea surface and headspace above were approximately 4.4 m^3 and 0.8 m^3, respectively. The headspace of each bag was sealed during the experiments, with the exception of sampling times and a few small holes that were left in the top of the mesocosm bags for gas exchange. In addition, the bags were covered by plastic domes to prevent rainfall and dust from entering and to minimize the likelihood of contamination. For each mesocosm bag, approximately 4400 L of natural seawater pumped from Wuyuan Bay was filtered through an ultrafiltration water purifier system (MU801-4T, Midea, China) equipped with 0.01-μm pore size cartridges (German-Made). The filtration device was equipped with automatic backwash system to avoid congestion. The pre-filtered water was then simultaneously allocated into each bag at the same flow rate within a period of 24 h. A known amount of NaCl solution was added to each bag to facilitate accurate determination of the volume of seawater in the bags based on the change of the salinity before and after salt addition[30]. The initial pCO_2 of the seawater in the bay

was about 650 μatm (pH = 7.6) because of the active decomposition of allochthonous organic matter by microbes. We set up three replicates of two distinct CO_2 partial pressures to simulate present and future conditions. To simulate a low pCO_2 level (LC, 400 μatm), approximately 2 L of Na_2CO_3 solution (~100 μmol kg^{-1}) was added to the LC treatments to accelerate the equilibrium between ambient air and seawater.[31] Meanwhile, an equal amount of Na_2CO_2 solution was added to the HC treatment to ensure that the total alkalinity was the same in both treatments. For the high pCO_2 treatment (HC, 1000 μatm), three bags were each supplemented with approximately 5 L of pre-filtered CO_2-saturated seawater.[32] Because the 5 L of CO_2-saturated seawater was only ~0.11% of the volume of seawater (~4400 L) in each mesocosm bag, the change in the total alkalinity of the HC treatment due to addition of the CO_2-saturated seawater was negligible. Throughout the experiment, air containing either 1000 μatm CO_2 (HC treatment) or 400 μatm CO_2 (LC treatment) was bubbled into the mesocosms via a CO_2 Enricher device (CE-100, Wuhan Ruihua Instrument & Equipment, China) at a flow rate of 4.8 L per minute. Three 13-cm-diameter air stone disks connected to 6-mm-diameter gas tubes were placed at the bottom of each bag to evenly disperse the air into the water column. The pore size of the air stones, 30–50 μm, was expected to produce bubbles with diameters of 0.40–0.45 mm [33] that would rise at rates of 0.09–0.11 m s^{-1}.[34] We assumed that direct injection of these small bubbles through the air stone disk did not alter mixing effects or disturb the plankton in the mesocosm. We inoculated the mesocosms with phytoplankton species that had

been studied extensively in the laboratory: two diatoms, *Phaeodactylum tricornuntum* (CCMA 106) and *Thalassiosira weissflogii* (CCMP 102), and the coccolithophorid *Emiliania huxleyi* (CS-369). The initial concentrations of *Phaeodactylum tricornuntum*, *Thalassiosira weissflogii*, and *Emiliania huxleyi* were 10, 10, and 20 cells mL^{-1}, respectively. The initial diatom/coccolithophorid cell ratio was therefore 1:1. Bacteria associated with the algal cultures were also introduced into the mesocosm along with the phytoplankton assemblages. The initial bacterial community was therefore similar in each mesocosm.[29]

Environmental Parameters

The temperature and salinity of the mesocosms were measured with a conductivity-temperature-depth sensor (RBR, Canada). Chemical parameters including pH, total alkalinity, dissolved inorganic carbon (DIC), dissolved organic carbon, and nutrients were measured every two days. The pH changes were measured with a pH meter (Benchtop pH510, OAKTON, USA) that was calibrated with National Bureau of Standards (NBS) buffer solutions (Hanna Instruments, USA). The DIC concentration was determined with a CO_2 analyzer (LI 7000, Apollo SciTech, USA), as described by Cai, et al.[35] The total alkalinity was determined by Gran titration. Reference materials from the laboratory of Andrew Dickson (CRM Batch 60#) were used to calibrate the system to a precision of ± 2 μmol kg^{-1} for DIC and total alkalinity.[35] The pCO_2 was

calculated from measured DIC and pH_{NBS} with the CO_2Sys Program [36] using the stoichiometric equilibrium constants for carbonic acid of Mehrbach, et al. [37] as refitted in different functional forms by Dickson and Millero.[38]

Chlorophyll *a*

Chlorophyll *a* (chl-*a*) concentrations were measured by high-performance liquid chromatography (HPLC) with a Shimadzu 20A HPLC system fitted with a 3.5-μm Eclipse XDB C_8 column (4.6 × 150 mm, Agilent Technologies, Waldbronn, Germany). Details of the procedure have been described by Liu, et al.[39] Briefly, samples for phytoplankton pigment analysis (0.2–2 L, according to biomass) were filtered through 25-mm GF/F glass fiber filters under a vacuum pressure of <75 mm Hg and in dim light. The filters were then immediately frozen (–80°C) until analysis in the laboratory (within 30 days). Phytoplankton pigments were extracted with N, N-dimethylformamide and analyzed with standards (DHI Water & Environment, Hørsholm, Denmark).

Abundance of Unattached Bacteria

Water samples (1.8 mL) for determination of cell numbers of the unattached bacteria were collected from each bag, immediately fixed with 1% (final concentration)

paraformaldehyde, and stored at −80°C until analysis. Bacterial abundance was quantified using an Accuri C6 flow cytometer (Becton, Dickinson, USA) under a 488-nm laser after staining with fluorochrome SYBR-Green 1.[40] Fluoresbrite carboxy YG 1.0-μm diameter microspheres were also added to the samples as an internal standard for the quantification of cell concentrations. Milli-Q water was used as a sheath fluid, and the event rate was between 100 and 400 cells mL^{-1} to avoid coincidence. Data acquisition and analysis were conducted with BD Accuri C6 Software (Becton, Dickinson, USA).

In vitro Oxygen-based Microbial Metabolism

Microbial metabolism was calculated from the changes of dissolved oxygen concentrations before and after 24-h incubations.[41] The dissolved oxygen concentration was measured by high-precision Winkler titration (Metrohm-848, Switzerland) for detection of the potentiometric end-point [42]. Water samples collected from each bag were transferred to 5-L polycarbonate bottles with a silicone tube and subsequently siphoned into calibrated 60-cm^3 borosilicate bottles. Initial oxygen concentrations were measured at the start of the incubations. Two sets of three light and three dark incubation bottles were placed in a large tank filled with water exposed to natural sunlight. The incubation temperature was maintained by running seawater. After the incubation, gross primary production (GPP) was equated to the difference

between the average dissolved oxygen concentrations in the light and dark bottles; community respiration (CR) was equated to the difference between the average dissolved oxygen concentrations in the initial and dark bottles. Measured GPP based on incubations in the large tank were assumed to be light-saturated rates (hereafter GPP_m). Estimates of in situ, depth-averaged gross primary production ($GPP_{in\text{-}situ}$) were made on the assumption that photosynthetic rates were a hyperbolic function of irradiance and the attenuation of light with depth was due to the absorption by phytoplankton pigments (Supporting Information methods). Net community production (NCP) was equated to the difference between $GPP_{in\text{-}situ}$ and CR.

The respiration rates of the unattached bacteria were estimated using water that had been pre-filtered (0.8 μm Nuclepore filter, Millipore) at a low negative pressure. The filtered water was dispensed into two sets of initial and dark bottles. The respiration rates of the unattached bacteria were equated to the difference between the average dissolved oxygen concentrations in the initial bottle and the dark bottle containing 0.8-μm–pre-filtered water. The large size respiration ($R_{>0.8\ \mu m}$) was equated to the difference between CR and the respiration rates of the unattached bacteria. We assumed that $R_{>0.8\ \mu m}$ was the sum of the respiration rates of the phytoplankton (PR) and attached bacteria because virtually no zooplankton passed through the ultrafiltration water purifier. PRs were assumed to be equal to 4.8% (LC treatment)

and 7.4 % (HC treatment) of the corresponding gross photosynthetic rates on the assumption that phytoplankton respiration rates were directly proportional to rates of photosynthesis [43, 44] and the fact that the phytoplankton populations that bloomed in the mesocosms were dominated by *Phaeodactylum tricornuntum*.[29] These percentages were estimated from the ratio of $R_{>0.8\ \mu m}$ to $GPP_{in\text{-}situ}$ on the day when that percentage was a minimum (day 11 for the LC treatment and day 9 for the HC treatment). We assumed that the respiration rates of the attached bacteria were negligible compared to PR at this time. These estimated percentages of PR in the LC and HC treatments are comparable to the results for *Phaeodactylum tricornuntum* under the similar pCO_2 conditions reported by Li, et al.[45] The difference between $R_{>0.8\ \mu m}$ and PR was equal to the respiration rates of the attached bacteria. Bulk bacterial respiration (BR) was then equated to the sum of the respiration rates contributed by both attached and unattached bacteria.

Changes of oxygen concentrations in triplicate incubation bottles collected from the same mesocosm were averaged to calculate the metabolic rate of one subsample. Rates of three subsamples from similar pCO_2 treatments were then combined to calculate median value and median absolute deviation for each sample day. In total, we had 96 estimates of each rate for the two treatments during the 16 sampling days. Oxygen-based metabolism was converted to a carbon basis using a respiratory

quotient of 0.9 on the assumption that inorganic nitrogen was released from organic matter in the form of ammonium.[46, 47]

Bulk Bacterial Production

Bulk bacterial production (BP) was determined with the ^{3}H-leucine incorporation method.[48] Four 1.8-mL aliquots of water were collected from each bag, added to 2-mL sterile microcentrifuge tubes (Axygen, Inc., USA), and incubated with a saturating concentration (10 nmol L^{-1}) of L-[3,4,5-^{3}H(N)]-Leucine (Perkin Elmer, USA) for 2 h in the dark. One sample was immediately killed by adding 100% trichloroacetic acid (TCA) as a control, and the other three were terminated with TCA at the end of the 2-h incubation. The water samples were filtered onto 0.2-μm polycarbonate filters (GE Water & Process Technologies, USA). The filters were rinsed twice with 3 mL of 5% TCA and twice with 2 mL of 80% ethanol before being frozen at –20°C. Upon return to the laboratory, the dried filters were placed in scintillation vials with 5 mL of Ultima Gold scintillation cocktail (Perkin-Elmer, USA). Radioactivity retained on the filters was measured as disintegrations per minute using a Tri-Carb 2800TR liquid scintillation counter (Perkin Elmer, USA). The rate of incorporation of ^{3}H leucine was calculated from the difference between the activities of the treatment and control tubes. We used a factor of 1.5 kg C mol leucine^{-1} to convert the incorporation of leucine to carbon equivalents, assuming no isotopic dilution.[48] Bacterial carbon

demand (BCD) was equated to bulk BP +bulk BR, and bacterial growth efficiency (BGE) was equated to bulk BP /BCD.[28]

Statistical Analyses

Two-sided Student's *t*-tests were used to determine whether average growth rates were significantly different from zero and to distinguish the different growth phases. The differences in the median values of each rate (e.g., GPP, bulk BP) between the two treatments were then tested by two-sided paired *t*-tests to examine effects of CO_2 enrichment during the different phases of the algal bloom. The data were log-transformed to satisfy the assumption of normality, which was confirmed (after transformation) via a Kolmogrov–Smirnov test. Differences were judged to be significant if the type I error rate (p) was less than 0.05. All statistical analyses were performed using SPSS (SPSS software, SPSS Inc., Chicago, USA).

Results

Initial Conditions and Phytoplankton Bloom Development

During the study period, water temperatures deviated by less than 1°C from a mean of 14.75°C, and the water in each bag was well mixed. Initial nitrate ($NO_2^- + NO_3^-$), ammonium (NH_4^+), phosphate (PO_4^{3-}), and silicate (SiO_3^{2-}) concentrations were 52–

54 μmol L^{-1}, 20–21 μmol L^{-1}, 2.4–2.6 μmol L^{-1}, and 38–41 μmol L^{-1}, respectively (Table 1). The total alkalinity values in the seawater were 2480 ± 56 μmol kg^{-1} (median value ± median absolute deviation, the same below) and 2470 ± 27 μmol kg^{-1} in the HC and LC treatments, respectively, on day 0 (Table 1). The pCO_2 of the seawater was higher in the HC treatment (1220 ± 150 μatm) than in the LC treatments (390 ± 54 μatm) initially (Figure 1a). Because of the high rates of bacterial respiration, the pCO_2 values increased (by approximately 300 μatm) during the first few days in both treatments (Figure 1a). Although air containing 1000 μatm CO_2 was continuously bubbled into the HC treatments, the pCO_2 values in both treatments decreased after day 6 because of rapid CO_2 uptake by the phytoplankton and were no longer different between the two treatments by day 16 (Figure 1a). Similar to the pCO_2 time series, the temporal variation of pH_{NBS} was driven by the high rates of biological activity. There was an initial decline in pH_{NBS} due to bacterial respiration and a subsequent increase as phytoplankton blooms developed (Figure 1a). In all the mesocosms, the development of a phytoplankton bloom led to a rapid decrease of nutrients. The nitrate concentrations dropped to very low levels of approximately 2.8 ± 0.3 μmol L^{-1} in the LC treatment and 5.8 ± 6.1 μmol L^{-1} in the HC treatment on day 15. At the end of the study, both phosphate and nitrate concentrations were close to their limits of detection. The initial DIC was higher in the HC treatment (2321 ± 5.8 μmol kg^{-1}) than in the LC treatment (2163 ± 24 μmol kg^{-1}) (Table 1). The DIC, like the pCO_2, increased in the first few days and then decreased as the algae grew.

[键入文字]

Table 1 Summary of initial characteristics of the mesocosms on day 0 (median ± median absolute deviation). The variation of temperature (Temp) indicates the diel cycle. The pH changes were measured with a pH meter that was calibrated with National Bureau of Standards (NBS) buffer solutions. HC: high pCO_2 level treatment. LC: low pCO_2 level treatment. DIC: dissolved inorganic carbon. TA: total alkalinity.

	Temp °C	Salinity psu	$NO_3^- + NO_2^-$ μmol L^{-1}	NH_4^+ μmol L^{-1}	PO_4^{3-} μmol L^{-1}	SiO_3^{2-} μmol L^{-1}	DIC μmol kg^{-1}	TA μmol kg^{-1}	pH_{NBS}	pCO_2 μatm
LC	15.5-17.2	29	54 ± 2.1	21 ± 2.6	2.6 ± 0.2	40 ± 2.2	2163 ± 24	2470 ± 27	8.2 ± 0.1	1220 ± 150
HC	15.5-17.2	29	53 ± 2.4	21± 2.3	2.5± 0.2	39 ± 0.5	2321 ± 5.8	2480 ± 56	7.8 ± 0.1	390 ± 54

After inoculation, phytoplankton pigment biomass in terms of chl-*a* increased rapidly (Figure 1b). The chl-*a* concentrations reached peaks of 385 ± 5.3 μg L^{-1} and 364 ± 31 μg L^{-1} in the LC (day 17) and HC (day 21) treatments, respectively (Figure 1b). Based on growth rates calculated from the natural logarithms of the chl-*a* concentrations (Figure 1b), two growth phases were initially identified: log phase (days 0–12), when average phytoplankton growth rates (0.7 ± 0.2 d^{-1} in the LC treatment and 0.7 ± 0.3 d^{-1} in the HC treatment) were similar in the two treatments and significantly greater than zero (p = 0.0010, *t*-test), and stationary phase (days 13–34), when average growth rates (0.0 ± 0.2 d^{-1} in the LC and –0.0 ± 0.3 d^{-1} in the HC treatment) were not significantly different from zero (p = 0.7492, *t*-test). The stationary phase was further

divided into two phases: stationary phase I (days 13–22) and stationary phase II (days 23–34), followed by the decline in the phytoplankton cell abundance after the peak during the stationary phase I [29]. Initial abundances of the unattached bacteria averaged $7.7 \pm 0.7 \times 10^6$ cells μL^{-1} and $7.6 \pm 0.1 \times 10^6$ cells μL^{-1} in the LC and HC treatments, respectively (Figure 1c). Thereafter, the abundances of the unattached bacteria dramatically decreased to minimal values on day 9 (Figure 1c), by which time phytoplankton populations had increased by roughly a factor of 400 (Figure 1b). Throughout the stationary phase, both chl-*a* concentrations and the abundances of the unattached bacteria remained relatively constant in the two treatments (Figure 1b and c). No significantly consistent differences between the abundances of the unattached bacteria and chl-*a* concentrations were apparent between the two treatments during either of the growth phases (Table 2).

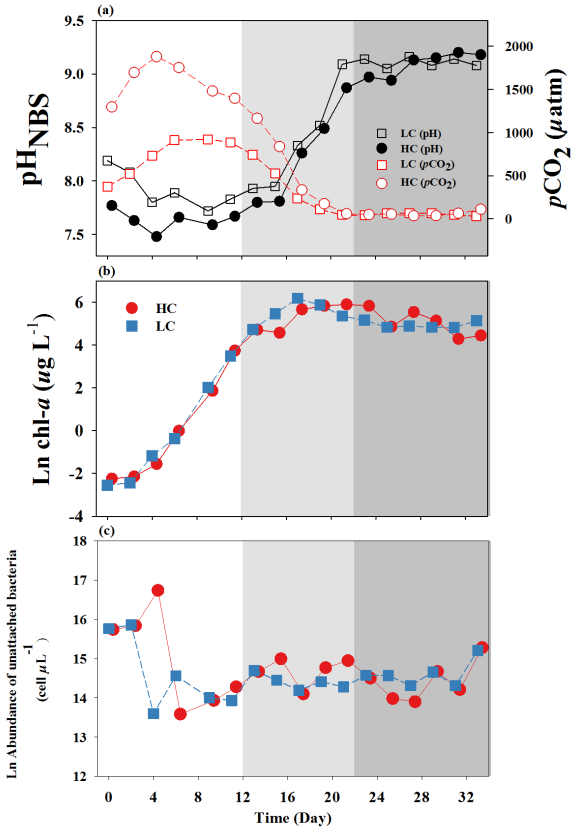

Figure 1. Temporal variations of (**a**) pCO_2 and pH_{NBS} in the seawater, (**b**) chlorophyll *a* (chl-*a*) and (**c**) abundance of the unattached bacteria in the high pCO_2 level (HC) and low pCO_2 level (LC) treatments. White, light grey and dark grey shaded area indicate the log phase, stationary phase I and stationary phase II of the phytoplankton bloom, respectively. The pH changes were measured with a pH meter that was calibrated with National Bureau of Standards (NBS) buffer solutions. Data are presented as medium values of three replicates for two treatments. The average median absolute deviation of pCO_2, pH_{NBS}, natural logarithm of chl-*a* and abundance of the unattached bacteria were 8.5 μatm, 0.1, 0.2 $\mu g\ L^{-1}$ and 0.2 cell μL^{-1}, respectively.

[键入文字]

Autotrophic Metabolism

$GPP_{in\text{-}situ}$ increased rapidly during the algal bloom and declined during the stationary phase (Figure 2a). Maxima of $GPP_{in\text{-}situ}$ were recorded near day 14 (Figure 2a). During stationary phase I, daily $GPP_{in\text{-}situ}$ in the HC treatment was 38% greater than in the LC treatment ($p = 0.0340$; Table 2). During stationary phase II, there was no significant difference between $GPP_{in\text{-}situ}$ in the HC and LC treatments (Figure 2a; Table 2). Productivity indices (i.e., the ratio of light-saturated GPP to chl-*a*) increased dramatically during the first few days of log-phase growth and reached maxima of roughly 5.3 g C g^{-1} chl-a^{-1} h^{-1} (Figure 2b). However, productivity indices declined rapidly during the second week of log phase growth and were <1 g C g^{-1} chl-a^{-1} h^{-1} throughout the stationary phase, an indication of extreme light and/or nutrient limitation (Figure 2b). During stationary phase I, productivity indices in the HC treatment were 39% higher than in the LC treatment ($p = 0.0277$; Table 2).

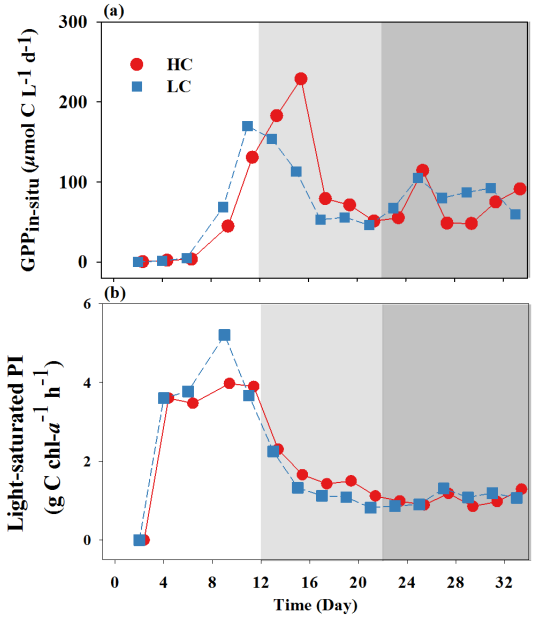

Figure 2. Temporal variations of (**a**) *in situ*, depth-averaged gross primary production ($GPP_{in\text{-}situ}$), (**b**) light-saturated productivity indices (PI, light-saturated GPP/ chlorophyll *a*) in the high pCO_2 level (HC) and low pCO_2 level (LC) treatments. White, light grey and dark grey shaded area indicate the log phase, stationary phase I and stationary phase II of the phytoplankton bloom, respectively. Data are presented as medium values of three replicates for two treatments. The average median absolute deviation of $GPP_{in\text{-}situ}$ and light-saturated PI were 15 μmol C L^{-1} d^{-1} and 0.3 g C chl-a^{-1} h^{-1}, respectively.

[键入文字]

Heterotrophic Bacterial Metabolism

Bulk BP increased dramatically from the log phase to stationary phase I and even further during stationary phase II (Figure 3a). There was no significant difference between bulk BP in the LC and HC treatments (Table 2). Bulk BR also increased dramatically between log phase and stationary phase (Figure 3b), but in the case of bulk BR there was a significant difference in the LC and HC treatments throughout stationary phase I ($p = 0.0058$; Table 2). Bulk BR was about 31% lower in the HC treatment during that time (Figure 3b). During the log phase, the attached and unattached bacteria accounted for roughly equal amounts of bulk BR, but during the stationary phase attached bacteria accounted for about 78% of bulk BR (Figure 3b). Similar to the response of bulk BR to the elevated CO_2 concentrations, significantly lower the respiration rates of attached and unattached bacteria were found in the LC treatment during days 13–22 ($p = 0.0041$ for the respiration rates of attached bacteria and $p = 0.0124$ for the respiration rates of attached bacteria; Table 2). BGE was relatively low (<5%) during the first eight days of the experiment and then increased until day 16 (Figure 4a). During days 13–22, BGEs were significantly higher in the HC treatment than that in the LC treatment ($p = 0.0127$; Table 2). There was no significantly consistent difference in BGEs between the two treatments during the log phase and stationary phase II (Table 2). In contrast, the BCD in the HC treatment was about 30% lower than that in the LC treatment during days 13–22 ($p = 0.0100$; Table

2). The BCD remained low during the start of the experiment and increased due to the elevations of bulk BP and bulk BR (Figure 4b).

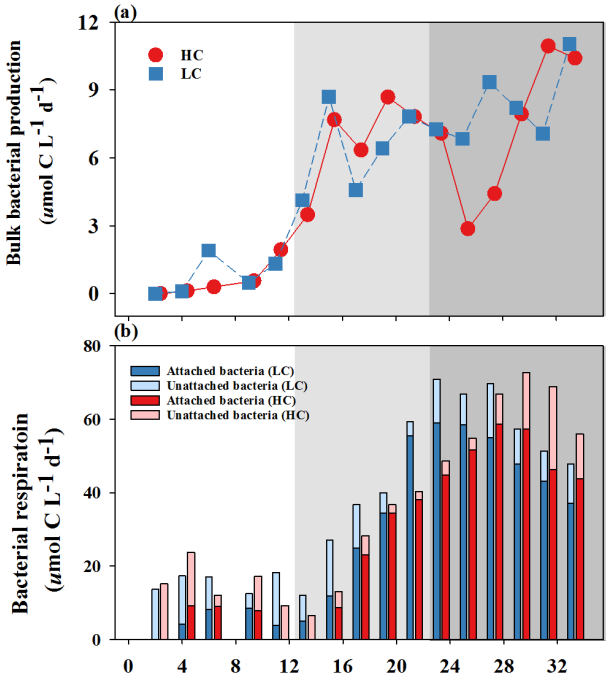

Figure 3. Temporal variations of (**a**) bulk bacterial production, (**b**) respiration of the attached and unattached bacteria, and bulk bacterial respiration in the high pCO_2 level (HC) and low pCO_2 level (LC) treatments. Style and color-coding as in Figure 2. The average median absolute deviation of bulk bacterial production, respiration of the attached bacteria, respiration of the unattached bacteria, and bulk bacterial respiration were 0.8 μmol C L^{-1} d^{-1}, 5.6 μmol C L^{-1} d^{-1}, 2.5 μmol C L^{-1} d^{-1}, and 6.1 μmol C L^{-1} d^{-1}, respectively.

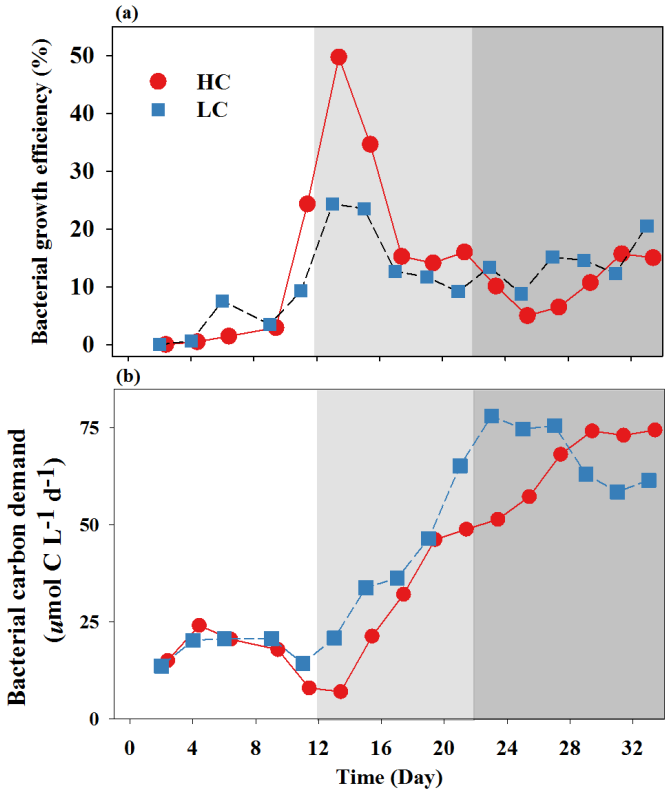

Figure 4. Temporal variations of (**a**) bacterial growth efficiency and (**b**) bacterial carbon demand in the high pCO_2 level (HC) and low pCO_2 level (LC) treatments. Style and color-coding as in Figure 2. The average median absolute deviation of bacterial growth efficiency and bacterial carbon demand were 2.0% and 6.2 μmol C L^{-1} d^{-1}, respectively.

Community Respiration and Metabolic Balance

Bulk BR accounted for a majority of CR in both treatments, but the contribution of bulk BR to CR was lower in the HC treatment than in the LC treatment (Figures 3b and 5a). Like bacterial abundance, CR trended down until day 9 (Figure 5a). It then

began to increase with the growth of phytoplankton until the end of sampling (Figure 5a). There was no significant difference of CR between the two treatments (Table 2).

Table 2. Type I error rates (*p* values) associated with comparisons between the low pCO_2 and high pCO_2 treatments of indicated parameters during the different phases of the phytoplankton bloom. Differences in median value of each parameter between the two pCO_2 treatments were conducted by two-sided pair *t*-tests. Significant effects are in bold.

	Log phase	Stationary phase I	Stationary phase II
	Days 0-12	**Days 13-22**	**Days 23-33**
Chlorophyll *a*	0.9112	0.4015	0.5204
Abundance of unattached bacteria	0.7157	0.0922	0.9127
Gross Primary Production (in-situ)	0.2591	**0.0340**	0.4223
Light-saturated productivity indices	0.8072	**0.0277**	0.8992
Bulk bacterial production	0.7778	0.1666	0.3335
Bulk bacterial respiration	0.2241	**0.0058**	0.4725.
Respiration of the attached bacteria	0.4752	**0.0041**	0.2394
Respiration of the unattached bacteria	0.5910	**0.0124**	0.7150
Bacterial growth efficiency	0.3936	**0.0127**	0.1713
Bacterial carbon demand	0.2248	**0.0100**	0.6851
Community respiration	0.7342.	0.4030	0.3214
Net community production	0.1412	**0.0020**	0.3211

In general, the temporal pattern of NCP was similar to that of $GPP_{in\text{-}situ}$ but offset by the contributions of CR (Figure 5b). NCP was negative (i.e., community metabolism was heterotrophic) for roughly the first week and last two weeks of the experiment (Figure 5b). On day 6, NCP became positive and peaked around days 14–16 (Figure 5b). Daily NCP was 45% higher in the HC treatments than in the LC treatments during stationary phase I ($p = 0.0020$; Table 2).

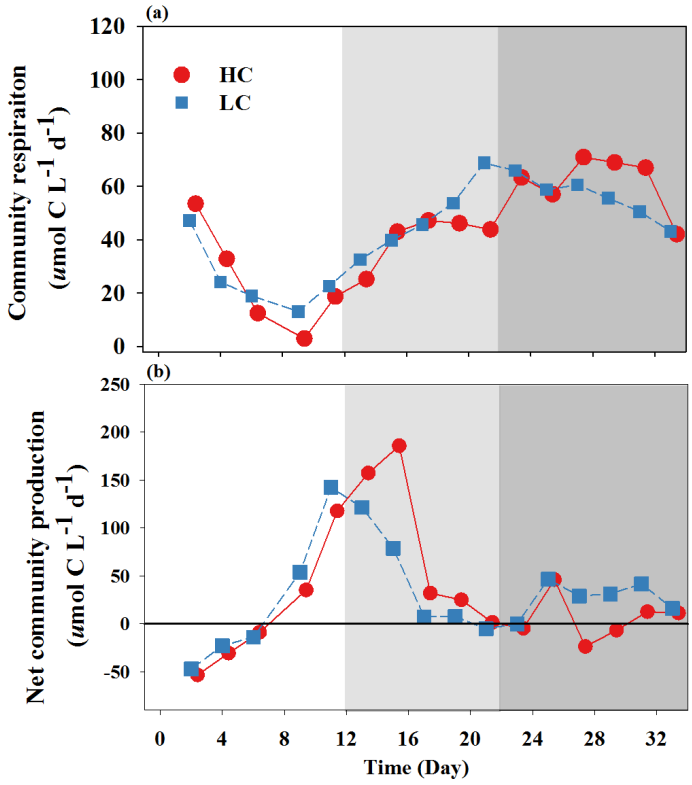

Figure 5. Temporal variations of **(a)** community respiration and (**b**) net community production in the high pCO_2 level (HC) and low pCO_2 level (LC) treatments. Style and color-coding as in Figure 2. The average median absolute deviation of community respiration and net community production were 7.8 μmol C L^{-1} d^{-1} and 22 μmol C L^{-1} d^{-1}, respectively.

Discussion

Responses of Autotrophic Metabolism

The effects of CO_2 fertilization on phytoplankton were most apparent during stationary phase I. During that time, *Phaeodactylum tricornuntum* accounted

[键入文字]

for >99% of the phytoplankton cells in the two treatments.[29] Previous studies have shown that elevated CO_2 either enhances, inhibits, or shows no measurable effect on the photosynthetic carbon fixation and/or growth of diatoms.[49] In this study, we found stimulation of $GPP_{in\text{-}situ}$ in the HC treatment under continuous supply of 1000 *u*atm CO_2 (Figure 2a and Table 2), which is coherent with the observation of enhanced ^{14}C-based net primary production and particular organic accumulation in this period.[29] Positive effects of OA similar to our observations have been reported in diatom monocultures,[50-52] mixed cultures,[53] and natural populations.[17] At the start of our experiment, when the phytoplankton bloom was developing, CO_2-related differences of phytoplankton metabolism were too small to be detected at a statistically significant level (Table 2). The time required for the differences to become large enough to be significant was probably related to the growth rate of the phytoplankton assemblages and the turnover time of the organic matter in the system.[54] The significantly higher productivity indices (the ratio of GPP_m to chl-*a*) in the HC treatment during stationary phase I (Figure 2b and Table 2) imply that the elevated primary production was due mainly to an increase in the efficiency of photosynthesis per chl-*a*. In the stationary phase, CCM activity may have been constrained by low light and the paucity of nitrogen for synthesis of CCM-specific proteins.[55] Assuming a chl-*a*–specific visible light absorption coefficient of 0.014 $m^2\ mg^{-1}$,[56] the average irradiance in the 2.5-m–deep water column during the stationary phase would have been only 8% of the surface irradiance at a chl-*a* concentration of 350 $\mu g\ L^{-1}$. With

CCM activity therefore constrained by lack of light and nitrogen, simple diffusion would have accounted for a relatively large percentage of CO_2 supply. Based on laboratory pH manipulation experiments, Riebesell, et al. [57] have pointed out that the flux of CO_2 to a cell's surface from diffusion depends on many factors, including the CO_2 concentration in the bulk medium, temperature, the cell radius, and the rate of chemical hydration of CO_2 by reaction with H_2O. During stationary phase, the CO_2 concentrations in the bulk medium would have played a major role in determining the rate of diffusion of CO_2 through the boundary layer around a cell because other conditions in the two treatments were very similar. The fact that the pCO_2 in the seawater decreased rapidly at the start of the stationary phase (Figure 1a) reflects the fact that photosynthetic carbon removal was faster than CO_2 dissolution into the seawater, the implication being that the phytoplankton cells became more sensitive to the difference of pCO_2 between the HC and LC treatments. At the start of stationary phase I on day 13, pCO_2 was still higher in the HC group (1260 ± 45 μatm) than in the LC group (753 ± 43 μatm) (Figure 1a). The higher CO_2 concentration in the HC treatment would have facilitated phytoplankton carbon uptake by enhancing the diffusion of CO_2 from the bulk medium to the cell surface. Interestingly, the enhancement of primary production lasted several days after there was no longer a difference of pCO_2 between the two treatments. Consistent with our observations, Taucher, Jones, James, Brzezinski, Carlson, Riebesell and Passow [53] also found that most of the significant effects of CO_2 enrichment on DIC uptake by two marine

diatoms occurred during stationary phase, when the inorganic carbon systems were similar, rather than during the time when the pCO_2 partial pressures were still close to target levels of 400 μatm and 1000 μatm. A mechanism responsible for these observations may be the allocation of energy savings from the down-regulation of CCMs during log phase of growth to the uptake and storage of nutrients and to the accumulation of intracellular ATP.[58] The greater accumulation of resources in the cells grown under HC conditions during the log phase would have made possible higher primary production rates during the subsequent time when nutrients were depleted and resource allocation became critical.[53]

Responses of Heterotrophic Bacterial Metabolism

In contrast to our hypothesis, we did not observe a significant stimulation of bulk BP concomitant with enhanced primary production (Figure 3a and Table 2). In this study, an empirical conversion factor of leucine-to-carbon was used to estimate the bulk BP in the two treatments, with the assumption that no effect of changes of pCO_2 on the conversion factors. This might, to some extent, mask the effects of CO_2 on bulk BP. Since nothing has been documented about effects of OA on the conversion factor of leucine-to-carbon, it is therefore impossible for us to determine the consequence of assuming a constant conversion factor. The conversion factor of leucine-to-carbon has been shown to increase from the open ocean to the coastal areas.[59, 60] Such patterns

along trophic gradients suggest that the conversion factor of leucine-to-carbon are functions of environmental conditions and depend in part on the composition of substrates and the bacterial community structure. Nevertheless, our mesocosm experiment was conducted with extremely eutrophic costal water. The conversion factors of leucine-to-carbon in the two treatments were considered similar to their maximal values, with little potential for increase. In addition, no significant differences in the bacterial communities between the two treatments were detected after day 9 in our study.[61] Therefore, differences of conversion factors related to the substrate supply and bacterial community between the HC and LC treatments were probably insignificant.

Interesting, there were a significant increase of BGE and reduction of bulk BR in the HC treatment throughout stationary phase I (Table 2). There have been few direct studies of pCO_2-related effects on bacterial respiration. The effect of increased CO_2 on bacterial respiration was first documented in the laboratory study of Teira, et al. [26], who reported a relatively constant bacterial production but a decline of the respiration rate of *Flavobacteriaceae* grown under a pCO_2 of 1000 μatm. In a natural community dominated by bacteria and picophytoplankton, Spilling, et al. [62] also observed an approximately 40% reduction in community respiration with increasing pCO_2. In contrast, no specific effects on bacterial respiration have been detected by direct

measurements in Artic waters.[28] At the present time, the typical pH in ocean surface waters (8.0–8.2) is higher than the intracellular pH (7.4–7.8) of bacteria.[63, 64] The energetic demands associated with this pH gradient include physiological processes such as membrane transport of H^+ or OH^-, enhanced expression of monovalent cation/proton antiporters, and increased acid production to sustain the homeostasis of the internal pH.[64, 65] A decrease of the pH in seawater due to OA would lead to an external pH closer to the bacterial intracellular pH and thereby reduce the metabolic cost (respiration) associated with internal pH regulation.[26, 62] Organisms require a relatively long time to acclimate to rapid changes of the chemical environment. Although the pH_{NBS} during the stationary phase increased to about 8.3 in the two treatments (Figure 1a), the decrease of BR in the HC treatment may have been related to acclimation to the 12 days of exposure to lower pH during the log phase. The reduction of bulk BR in the HC treatment resulted in a higher BGE and lower BCD (Figure 4a-b and Table 2), the result being that a higher percentage of assimilated carbon was transformed into bacterial biomass and less was lost to respiration in the HC treatment compared to the LC treatment. This result is qualitatively very similar to the effects of elevated pCO_2 on *Flavobacteriaceae* previously reported by Teira, et al. [26]. The implication is that transfer of carbon to higher trophic levels through the microbial loop [66, 67] under future OA conditions would be more efficient than the present case.

The relative contributions of attached and unattached bacteria to bulk BR found in this study are very similar with a previous report by Smith, et al. [68], who found that diatoms were colonized by bacteria throughout a diatom bloom in a mesocosm, and although greatly outnumbered by unattached bacteria, the attached bacteria were generally responsible for a majority of the BCD. Although attached and unattached bacteria contributed about equally to bulk BR during the log phase of our study, the fact that attached bacteria contributed 78% of the bulk BR during the stationary phase is very consistent with the Smith et al.[68]

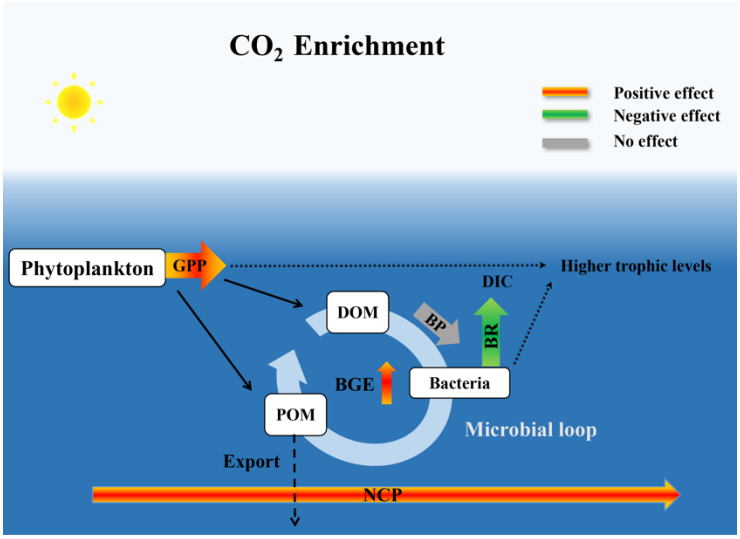

Figure 6. A schematic illustrating the responses of microbial metabolism under the CO_2 enrichment. According to our findings, rising CO_2 leads to enhanced gross primary production and decline in bacterial respiration. Few effects occur in the bacterial production. Together, these changes increase the net community production at the community level. Additionally, the reduce in the bacterial respiration but constant bacterial production result in an elevation of bacterial growth efficiency, implying with more carbon into bacterial biomass rather than loss in terms of CO_2. GPP: gross primary production. BP: bacterial production. BR: bacterial respiration. BGE: bacterial growth efficiency. NCP: net community production. POM: particulate organic matter. DOM: dissolved organic matter. DIC: dissolved inorganic carbon.

Response of Community Metabolism and Implications

We observed a significant (45%) increase of NCP (Figure 5b and Table 2) during stationary phase I as a result of the enhancement of $GPP_{in\text{-}situ}$ and the decline of bulk BR in the HC treatment. Changes of CR were statistically insignificant (Figure 5a and Table 2) because the lower bulk BR in the HC treatment was offset by the higher rate of PR, which reflected the enhancement of photosynthetic rates by the elevated pCO_2. The elevation of NCP during stationary phase I suggests that CO_2 enrichment may have a profound impact on the net flux of carbon, with more organic matter accumulation under CO_2-enriched conditions (Figure 6). However, because of the lack of zooplankton in our system, it is possible that in a natural system much of this additional organic carbon would be lost to respiration at higher trophic levels or exported to the interior of the ocean via the biological pump. In addition, the diversity of phytoplankton and bacteria in our mesocosms was very different from that of a natural community. Thus extrapolating the results of the present work to more natural systems should be done with caution.

Conclusions

The impacts of CO_2 enrichment on microbial autotrophic and heterotrophic carbon metabolism were evaluated in subtropical coastal mesocosms that were manipulated by continuous bubbling with air containing either 1000 or 400 μatm CO_2. The effect

of CO_2 enrichment was to enhance NCP for a period of about two weeks. The statistically significant elevation of NCP via CO_2 enrichment was due to an increase of primary production and decrease of bacterial respiration. The simultaneous responses of both autotrophic and heterotrophic organisms to CO_2 enrichment implies that comprehensive studies, especially of bacterial metabolism, will be needed in the future to elucidate the interactions that determine how marine systems change in response to OA. Because coastal regions are especially vulnerable to environmental perturbations such as eutrophication [69] and hypoxia,[70] their interactions with global ocean acidification may lead to unprecedented complexity.

Supporting Information

Appendix. Methods Estimation of *in situ* photosynthetic rates

Author Contributions:

Conceived and designed the experiments: Kunshan Gao, YiBin Huang, Xin Liu, Yaping Wu, Banqing Huang; Performed the experiments: Yibin Huang, Xin Liu, Ya Li, Yaping Wu; Analyzed the data: Yibin Huang, Edward A. Laws, Yuyuan Xie;

Wrote the paper: Yibin Huang, Xin Liu; Revised the manuscript: Xin Liu, Edward A. Laws, Binzhang Chen, Bangqin Huang, Kunshan Gao

The authors declare no competing financial interest.

Acknowledgments

This work was supported mainly by grants from the National Key Research and Development Program (No.2016YFA0601203) and the China NSF (No. 41330961, 41430967, 41720104005, U1406403). We thank Tifeng Wang, Nana Liu, Futian Li, Peng Jin, Ruiping Huang, Shanying Tong, Xin Lin, and Xiangqi Yi, Xianglan Zeng, whom made contributions to the mesocosm experiments.

References

This article references 70 other publications.

1. Doney, S. C.; Fabry, V. J.; Feely, R. A.; Kleypas, J. A., Ocean acidification: the other CO_2 problem. *Annual Review of Marine Science* **2009,** *1*, 169-92.
2. Caldeira, K.; Wickett, M. E., Oceanography: anthropogenic carbon and ocean pH. *Nature* **2003,** *425*, (6956), 365-365.
3. Feely, R. A.; Sabine, C. L.; Lee, K.; Berelson, W.; Kleypas, J.; Fabry, V. J.; Millero, F. J., Impact of anthropogenic CO2 on the CaCO3 system in the oceans. *Science* **2004,** *305*, (5682), 362-366.
4. Gattuso, J. P.; Magnan, A.; Bille, R.; Cheung, W. W. L.; Howes, E. L.; Joos, F.; Allemand, D.; Bopp, L.; Cooley, S. R.; Eakin, C. M.; Hoegh-Guldberg, O.; Kelly, R. P.; Portner, H. O.; Rogers, A. D.; Baxter, J. M.; Laffoley, D.; Osborn, D.; Rankovic, A.; Rochette, J.; Sumaila, U. R.; Treyer, S.; Turley, C., Contrasting futures for ocean and society from different anthropogenic CO_2 emissions scenarios. *Science* **2015,** *349*, (6243), aac4722.
5. Feely, R. A.; Alin, S. R.; Newton, J.; Sabine, C. L.; Warner, M.; Devol, A.; Krembs, C.; Maloy, C., The combined effects of ocean acidification, mixing, and respiration on pH and carbonate saturation in an urbanized estuary. *Estuarine, Coastal and Shelf Science* **2010,** *88*, (4), 442-449.
6. Cai, W.-J.; Hu, X.; Huang, W.-J.; Murrell, M. C.; Lehrter, J. C.; Lohrenz, S. E.;

Chou, W.-C.; Zhai, W.; Hollibaugh, J. T.; Wang, Y., Acidification of subsurface coastal waters enhanced by eutrophication. *Nature Geoscience* **2011,** *4*, (11), 766-770.
7. Mucci, A.; Starr, M.; Gilbert, D.; Sundby, B., Acidification of lower St. Lawrence Estuary bottom waters. *Atmosphere-Ocean* **2011,** *49*, (3), 206-218.
8. Behrenfeld, M. J.; Falkowski, P. G., Photosynthetic rates derived from satellite-based chlorophyll concentration. *Limnology and Oceanography* **1997,** *42*, (1), 1-20.
9. Del Giorgio, P.; Cole, J., Bacterial energetics and growth efficiency. *Microbial Ecology of the Oceans. Wiley-Liss* **2000**, 289-325.
10. Wannicke, N.; Endres, S.; Engel, A.; Grossart, H.-P.; Nausch, M.; Unger, J.; Voss, M., Response of Nodularia spumigena to pCO_2-Part 1: growth, production and nitrogen cycling. *Biogeosciences* **2012,** *9*, (8), 2973.
11. Riebesell, U.; Gattuso, J. P.; Thingstad, T. F.; Middelburg, J. J., "Arctic ocean acidification: pelagic ecosystem and biogeochemical responses during a mesocosm study" Preface. *Biogeosciences* **2013,** *10*, (8), 5619-5626.
12. Dutkiewicz, S.; Morris, J. J.; Follows, M. J.; Scott, J.; Levitan, O.; Dyhrman, S. T.; Berman-Frank, I., Impact of ocean acidification on the structure of future phytoplankton communities. *Nature Climate Change* **2015,** *5*, (11), 1002-1006.
13. Hopkinson, B. M.; Dupont, C. L.; Allen, A. E.; Morel, F. M., Efficiency of the CO_2-concentrating mechanism of diatoms. *Proc Natl Acad Sci U S A* **2011,** *108*, (10), 3830-7.
14. Portner, H. O.; Farrell, A. P., Ecology. Physiology and climate change. *Science* **2008,** *322*, (5902), 690-2.
15. Hein, M.; SandJensen, K., CO_2 increases oceanic primary production. *Nature* **1997,** *388*, (6642), 526-527.
16. Iglesias-Rodriguez, M. D.; Halloran, P. R.; Rickaby, R. E.; Hall, I. R.; Colmenero-Hidalgo, E.; Gittins, J. R.; Green, D. R.; Tyrrell, T.; Gibbs, S. J.; von Dassow, P.; Rehm, E.; Armbrust, E. V.; Boessenkool, K. P., Phytoplankton calcification in a high-CO_2 world. *Science* **2008,** *320*, (5874), 336-40.
17. Riebesell, U.; Schulz, K. G.; Bellerby, R. G.; Botros, M.; Fritsche, P.; Meyerhofer, M.; Neill, C.; Nondal, G.; Oschlies, A.; Wohlers, J.; Zollner, E., Enhanced biological carbon consumption in a high CO_2 ocean. *Nature* **2007,** *450*, (7169), 545-8.
18. Feng, Y.; Warner, M. E.; Zhang, Y.; Sun, J.; Fu, F.-X.; Rose, J. M.; Hutchins, D. A., Interactive effects of increased pCO_2, temperature and irradiance on the marine coccolithophore *Emiliania huxleyi* (Prymnesiophyceae). *European Journal of Phycology* **2009,** *43*, (1), 87-98.
19. Tortell, P. D.; Morel, F. M. M., Sources of inorganic carbon for phytoplankton in the eastern Subtropical and Equatorial Pacific Ocean. *Limnology and Oceanography* **2002,** *47*, (4), 1012-1022.
20. Gao, K. S.; Zheng, Y. Q., Combined effects of ocean acidification and solar UV radiation on photosynthesis, growth, pigmentation and calcification of the coralline alga *Corallina sessilis* (Rhodophyta). *Global Change Biology* **2010,** *16*, (8), 2388-2398.
21. Rokitta, S. D.; Rost, B., Effects of CO_2 and their modulation by light in the life-
[键入文字]

cycle stages of the coccolithophore *Emiliania huxleyi*. *Limnology and Oceanography* **2012,** *57*, (2), 607-618.
22. Liu, J. W.; Weinbauer, M. G.; Maier, C.; Dai, M. H.; Gattuso, J. P., Effect of ocean acidification on microbial diversity and on microbe-driven biogeochemistry and ecosystem functioning. *Aquatic Microbial Ecology* **2010,** *61*, (3), 291-305.
23. Grossart, H. P.; Allgaier, M.; Passow, U.; Riebesell, U., Testing the effect of CO_2 concentration on the dynamics of marine heterotrophic bacterioplankton. *Limnology and Oceanography* **2006,** *51*, (1), 1-11.
24. Rochelle-Newall, E.; Delille, B.; Frankignoulle, M.; Gattuso, J.-P.; Jacquet, S.; Riebesell, U.; Terbrüggen, A.; Zondervan, I., Chromophoric dissolved organic matter in experimental mesocosms maintained under different pCO_2 levels. *Marine Ecology Progress Series* **2004,** *272*, 25-31.
25. Bunse, C.; Lundin, D.; Karlsson, C. M. G.; Akram, N.; Vila-Costa, M.; Palovaara, J.; Svensson, L.; Holmfeldt, K.; Gonzalez, J. M.; Calvo, E.; Pelejero, C.; Marrase, C.; Dopson, M.; Gasol, J. M.; Pinhassi, J., Response of marine bacterioplankton pH homeostasis gene expression to elevated CO_2. *Nature Climate Change* **2016,** *6*, (5), 483-487.
26. Teira, E.; Fernandez, A.; Alvarez-Salgado, X. A.; Garcia-Martin, E. E.; Serret, P.; Sobrino, C., Response of two marine bacterial isolates to high CO_2 concentration. *Marine Ecology Progress Series* **2012,** *453*, 27-36.
27. Coffin, R. B.; Montgomery, M. T.; Boyd, T. J.; Masutani, S. M., Influence of ocean CO_2 sequestration on bacterial production. *Energy* **2004,** *29*, (9-10), 1511-1520.
28. Motegi, C.; Tanaka, T.; Piontek, J.; Brussaard, C. P. D.; Gattuso, J. P.; Weinbauer, M. G., Effect of CO_2 enrichment on bacterial metabolism in an Arctic fjord. *Biogeosciences* **2013,** *10*, (5), 3285-3296.
29. Liu, N.; Tong, S.; Yi, X.; Li, Y.; Li, Z.; Miao, H.; Wang, T.; Li, F.; Yan, D.; Huang, R., Carbon assimilation and losses during an ocean acidification mesocosm experiment, with special reference to algal blooms. *Marine Environmental Research* **2017,** *129*, 229-235.
30. Czerny, J.; Schulz, K. G.; Ludwig, A.; Riebesell, U., Technical Note: A simple method for air–sea gas exchange measurements in mesocosms and its application in carbon budgeting. *Biogeosciences* **2013,** *10*, (3), 1379-1390.
31. Albright, R.; Caldeira, L.; Hosfelt, J.; Kwiatkowski, L.; Maclaren, J. K.; Mason, B. M.; Nebuchina, Y.; Ninokawa, A.; Pongratz, J.; Ricke, K. L.; Rivlin, T.; Schneider, K.; Sesboue, M.; Shamberger, K.; Silverman, J.; Wolfe, K.; Zhu, K.; Caldeira, K., Reversal of ocean acidification enhances net coral reef calcification. *Nature* **2016,** *531*, (7594), 362-5.
32. Riebesell, U.; Czerny, J.; von Brockel, K.; Boxhammer, T.; Budenbender, J.; Deckelnick, M.; Fischer, M.; Hoffmann, D.; Krug, S. A.; Lentz, U.; Ludwig, A.; Muche, R.; Schulz, K. G., Technical Note: A mobile sea-going mesocosm system - new opportunities for ocean change research. *Biogeosciences* **2013,** *10*, (3), 1835-1847.
33. Parthasarathy, R.; Ahmed, N., Size distribution of bubbles generated by fine-pore

spargers. *Journal of Chemical Engineering of Japan* **1996,** *29*, (6), 1030-1034.
34. Martínez, I.; Casas, P., Simple model for CO2 absorption in a bubbling water column. *Brazilian Journal of Chemical Engineering* **2012,** *29*, (1), 107-111.
35. Cai, W.-J.; Dai, M.; Wang, Y.; Zhai, W.; Huang, T.; Chen, S.; Zhang, F.; Chen, Z.; Wang, Z., The biogeochemistry of inorganic carbon and nutrients in the Pearl River estuary and the adjacent Northern South China Sea. *Continental Shelf Research* **2004,** *24*, (12), 1301-1319.
36. Pierrot, D.; Lewis, E.; Wallace, D., MS Excel program developed for CO2 system calculations. *Carbon Dioxide Information Analysis Center, Oak Ridge National Laboratory, US Department of Energy* **2006**.
37. Mehrbach, C.; Culberson, C. H.; Hawley, J. E.; Pytkowicx, R. M., Measurement of the apparent dissociation constants of carbonic acid in seawater at atmospheric pressure. *Limnology and Oceanography* **1973,** *18*, (18), 897-907.
38. Dickson, A.; Millero, F. J., A comparison of the equilibrium constants for the dissociation of carbonic acid in seawater media. *Deep Sea Research Part I* **1987,** *34*, (10), 1733-1743.
39. Liu, X.; Huang, B.; Huang, Q.; Wang, L.; Ni, X.; Tang, Q.; Sun, S.; Wei, H.; Liu, S.; Li, C., Seasonal phytoplankton response to physical processes in the southern Yellow Sea. *Journal of Sea Research* **2015,** *95*, 45-55.
40. Marie, D.; Partensky, F.; Jacquet, S.; Vaulot, D., Enumeration and cell cycle analysis of natural populations of marine picoplankton by flow cytometry using the nucleic acid stain SYBR Green I. *Applied and Environmental Microbiology* **1997,** *63*, (1), 186-193.
41. Serret, P.; Fernandez, E.; Sostres, J. A.; Anadon, R., Seasonal compensation of microbial production and respiration in a temperate sea. *Marine Ecology Progress Series* **1999,** *187*, 43-57.
42. Oudot, C.; Gerard, R.; Morin, P.; Gningue, I., Precise shipboard determination of dissolved-oxygen (Winkler procedure) for productivity studies with a commercial system. *Limnology and Oceanography* **1988,** *33*, (1), 146-150.
43. Laws, E. A.; Bannister, T. T., Nutrient- and light-limited growth of *Thalassiosira fluviatilis* in continuous culture with implications for phytoplankton growth in the ocean. *Limnology and Oceanography* **1980,** *25*, (3), 457-473.
44. Laws, E.; Caperon, J., Carbon and nitrogen metabolism by Monochrysis lutheri: Measurement of growth-rate-dependent respiration rates. *Marine Biology* **1976,** *36*, (1), 85-97.
45. Li, F.; Beardall, J.; Collins, S.; Gao, K., Decreased photosynthesis and growth with reduced respiration in the model diatom Phaeodactylum tricornutum grown under elevated CO_2 over 1800 generations. *Global Change Biology* **2017,** *23*, (1), 127-137.
46. Laws, E. A., Photosynthetic quotients, new production and net community production in the open ocean. *Deep Sea Research Part I* **1991,** *38*, (1), 143-167.
47. Hedges, J. I.; Baldock, J. A.; Gélinas, Y.; Lee, C.; Peterson, M. L.; Wakeham, S. G., The biochemical and elemental compositions of marine plankton: A NMR

perspective. *Marine Chemistry* **2002,** *78*, (1), 47-63.
48. Kirchman, D., Leucine incorporation as a measure of biomass production by heterotrophic bacteria. *Handbook of Methods in Aquatic Microbial Ecology. Lewis* **1993**, 509-512.
49. Gao, K.; Campbell, D. A., Photophysiological responses of marine diatoms to elevated CO_2 and decreased pH: a review. *Functional Plant Biology* **2014,** *41*, (5), 449-459.
50. Chen, X. W.; Gao, K. S., Characterization of diurnal photosynthetic rhythms in the marine diatom *Skeletonema costatum* grown in synchronous culture under ambient and elevated CO_2. *Functional Plant Biology* **2004,** *31*, (4), 399-404.
51. Li, Y.; Xu, J.; Gao, K., Light-modulated responses of growth and photosynthetic performance to ocean acidification in the model diatom *Phaeodactylum tricornutum*. *PLoS One* **2014,** *9*, (5), e96173.
52. Wu, Y.; Gao, K.; Riebesell, U., CO_2-induced seawater acidification affects physiological performance of the marine diatom *Phaeodactylum tricornutum*. *Biogeosciences* **2010,** *7*, (9), 2915-2923.
53. Taucher, J.; Jones, J.; James, A.; Brzezinski, M. A.; Carlson, C. A.; Riebesell, U.; Passow, U., Combined effects of CO_2 and temperature on carbon uptake and partitioning by the marine diatoms Thalassiosira weissflogii and Dactyliosolen fragilissimus. *Limnology and Oceanography* **2015,** *60*, (3), 901-919.
54. Schulz, K. G.; Bellerby, R. G. J.; Brussaard, C. P. D.; Budenbender, J.; Czerny, J.; Engel, A.; Fischer, M.; Koch-Klavsen, S.; Krug, S. A.; Lischka, S.; Ludwig, A.; Meyerhofer, M.; Nondal, G.; Silyakova, A.; Stuhr, A.; Riebesell, U., Temporal biomass dynamics of an Arctic plankton bloom in response to increasing levels of atmospheric carbon dioxide. *Biogeosciences* **2013,** *10*, (1), 161-180.
55. Giordano, M.; Beardall, J.; Raven, J. A., CO_2 concentrating mechanisms in algae: mechanisms, environmental modulation, and evolution. *Annual Reviews of Plant Biology* **2005,** *56*, 99-131.
56. Atlas, D.; Bannister, T., Dependence of mean spectral extinction coefficient of phytoplankton on depth, water color, and species. *Limnology and Oceanography* **1980,** *25*, (1), 157-159.
57. Riebesell, U.; Wolfgladrow, D. A.; Smetacek, V., Carbon-Dioxide Limitation of Marine-Phytoplankton Growth-Rates. *Nature* **1993,** *361*, (6409), 249-251.
58. Spungin, D.; Berman-Frank, I.; Levitan, O., *Trichodesmium*'s strategies to alleviate phosphorus limitation in the future acidified oceans. *Environmental Microbiology* **2014,** *16*, (6), 1935-47.
59. Alonso-Sáez, L.; Gasol, J. M.; Arístegui, J.; Vilas, J. C.; Vaqué, D.; Duarte, C. M.; Agustí, S., Large-scale variability in surface bacterial carbon demand and growth efficiency in the subtropical northeast Atlantic Ocean. *Limnology and Oceanography* **2007,** *52*, (2), 533-546.
60. Calvo-Díaz, A.; Morán, X. A. G., Empirical leucine-to-carbon conversion factors for estimating heterotrophic bacterial production: seasonality and predictability in a

temperate coastal ecosystem. *Applied and Environmental Microbiology* **2009,** *75*, (10), 3216.
61. Lin, X.; Huang, R.; Li, Y.; Wu, Y.; Hutchins, D. A.; Dai, M.; Gao, K., Insignificant effects of elevated CO_2 on bacterioplankton community in a eutrophic coastal mesocosm experiment. *Biogeosciences Discussions* **2017**, 1-36.
62. Spilling, K.; Paul, A. J.; Virkkala, N.; Hastings, T.; Lischka, S.; Stuhr, A.; Bermudez, R.; Czerny, J.; Boxhammer, T.; Schulz, K. G.; Ludwig, A.; Riebesell, U., Ocean acidification decreases plankton respiration: evidence from a mesocosm experiment. *Biogeosciences* **2016,** *13*, (16), 4707-4719.
63. Booth, I. R., Regulation of cytoplasmic pH in bacteria. *Microbiological Reviews* **1985,** *49*, (4), 359-78.
64. Padan, E.; Bibi, E.; Ito, M.; Krulwich, T. A., Alkaline pH homeostasis in bacteria: new insights. *Biochimica et biophysica acta (BBA)-biomembranes* **2005,** *1717*, (2), 67-88.
65. Smith, F. A.; Raven, J. A., Intracellular pH and its regulation. *Annual Review of Plant Physiology* **1979,** *30*, (1), 289-311.
66. Ducklow, H., Bacterial production and biomass in the oceans. *Microbial Ecology of the Oceans* **2000,** *1*, 85-120.
67. Azam, F.; Fenchel, T.; Field, J. G.; Gray, J. S.; Meyerreil, L. A.; Thingstad, F., The ecological role of water-column microbes in the sea. *Marine Ecology Progress Series* **1983,** *10*, (3), 257-263.
68. Smith, D. C.; Steward, G. F.; Long, R. A.; Azam, F., Bacterial mediation of carbon fluxes during a diatom bloom in a mesocosm. *Deep Sea Research Part II: Topical Studies in Oceanography* **1995,** *42*, (1), 75-97.
69. Borgesa, A. V.; Gypensb, N., Carbonate chemistry in the coastal zone responds more strongly to eutrophication than ocean acidification. *Limnology and Oceanography* **2010,** *55*, (1), 346-353.
70. Wang, H.; Dai, M.; Liu, J.; Kao, S. J.; Chao, Z.; Cai, W. J.; Wang, G.; Wei, Q.; Zhao, M.; Sun, Z., Eutrophication-Driven Hypoxia in the East China Sea off the Changjiang Estuary. *Environmental Science & Technology* **2016,** *50*, (5), 2255.